ELSEVIER

Thin Solid Films 384 (2001) 37–45

thin solid films

www.elsevier.com/locate/tsf

Determination of the thickness of thin silane films on aluminium surfaces by means of spectroscopic ellipsometry

A. Franquet*[,a], J. De Laet[a], T. Schram[a], H. Terryn[a], V. Subramanian[b], W.J. van Ooij[b], J. Vereecken[a]

[a] *Department of Metallurgy, Electrochemistry and Materials Science, Vrije Universiteit Brussel, Pleinlaan 2, B-1050 Brussels, Belgium*
[b] *Department of Materials Science and Engineering, University of Cincinnati, Cincinnati, OH 45221-0012, USA*

Received 13 April 2000; received in revised form 1 September 2000; accepted 9 October 2000

Abstract

The thickness of thin films of non-functional silane bis-1,2-(triethoxysilyl)ethane $(H_5C_2O)_3Si\text{-}CH_2CH_2\text{-}Si(OC_2H_5)_3$ (BTSE) deposited on aluminium surfaces is investigated using spectroscopic ellipsometry (250–1700 nm). The data processing of the ellipsometry spectra is carried out by means of simulation and regression techniques. New advances in data processing, e.g. multiple sample analysis and determination of thickness non-uniformity, are applied to characterise these thin polymer films realistically. The influence of the concentration of the BTSE solution and the curing of the film is investigated. Optical thickness estimates are corroborated by independent auger electron spectroscopy and transmission electron microscopy analysis.

Keywords: Silane; Thickness; Spectroscopic ellipsometry; Aluminium

1. Introduction

The use of hexavalent chromium for surface treatment of metals has a long and distinguished history. However, for both environmental and worker safety reasons, the replacement of this hexavalent chromium treatment became a major priority and research and development activities increased to develop alternative non-toxic treatment processes.

In particular, the application of silane coupling agents to metals has demonstrated its potential as adhesion-promoting [1] and corrosion-inhibiting [2] pre-treatments and seems to give promising results compared to the undesirable chromate treatment. Organofunctional silanes are hybrid organic–inorganic compounds that can be used as coupling agents across the organic–inorganic interface [1]. The commonly used silane coupling agents have the structure $X_3Si(CH_2)_nY$, where X represents a hydrolysable group such as methoxy or ethoxy and Y an organofunctional group such as chlorine, amine, epoxy or mercapto. Non-functional silanes are very similar to functional silanes in their structure, except that they have hydrolysable Si–O–C bonds on both ends of the carbon chain, and are better known as cross-linking agents.

Various organofunctional silanes are available on the market today (Table 1). Applied on different metallic substrates, they have been widely studied in the past from both a formation and a performance point of view. As proposed by Plueddemann [1], organofunctional silanes can bond to the metallic surface via the formation of oxane bonds induced by the interaction of silanol groups with the metal oxide surface. This reaction can be expressed by the general equation

$$Me\text{–}O\text{–}Si + H_2O \rightleftarrows Me\text{–}O\text{–}H + H\text{–}O\text{–}Si\text{–} \quad (1)$$

* Corresponding author. Tel.: +32-2-6293536; fax: +32-2-6293200.
E-mail address: afranque@vub.ac.be (A. Franquet).

0040-6090/01/$ - see front matter
PII: S0040-6090(00)01805-8

Table 1
Representative list of commercial silanes

Abbreviation	Chemical formula and name
γ-APS	$H_2NCH_2CH_2CH_2Si(OCH_2CH_3)_3$ [gamma-aminopropyltriethoxysilane]
CPS	$ClCH_2CH_2CH_2Si(OCH_3)_3$ [chloropropyl-trimethoxysilane]
EPS	$CH_2OCHCH_2O(CH_2)_3Si(OCH_3)_3$ [3-glycidoxypropyltrimethoxysilane]
γ-UPS	$NH_2C(=O)NHCH_2CH_2CH_2Si(OCH_3)_x(OC_2H_5)_{3-x}$ [gamma-ureidopropyltrialkoxysilane]
γ-MCPS	$HSCH_2CH_2CH_2Si(OCH_3)_3$ [gamma-mercaptopropyltrimethoxysilane]
VS	$CH_2=CHSi(OCH_3)_3$ [vinyltrimethoxysilane]

The literature provides many studies, performed on different systems, which confirm this interaction [3–6]. However, in some cases, and especially with aminosilanes, the coupling agents tend to adsorb onto metal surface with an inverted orientation and therefore three kinds of reactions can be found (Fig. 1) [7]. (a) and (b) orientations do not permit good performances for metal and paint adhesions and corrosion protection. For this reason, a two-step process was proposed in the case of the application of paint coatings on a metallic substrate [8], which has given promising results on steel [9] and aluminium [10] in terms of improved corrosion performance. This treatment involves sequential rinses with non-functional silane such as BTSE (bis-1,2-(triethoxysilyl)ethane) coated on metal and a choice functional silane.

Concerning the BTSE molecules applied on Al surfaces, some papers report the process parameters and coating conditions [11], corrosion and adhesion performances determined by salt spray and salt water immersion testing and electrochemical impedance spectroscopy (EIS) measurements [10]. Nevertheless, concerning the characterisation of BTSE/metal systems, there is a lack of information in the literature. One of the important aspects in current understanding of silane-based conversion processes is the knowledge of the thickness of the BTSE films and its dependence on deposition conditions such as bath concentration, immersion time and curing. The purpose of this paper was therefore to perform a first systematic and quantitative study of the film thickness of BTSE coatings applied on aluminium. To this end, spectroscopic ellipsometry (SE) has been applied [12]. To confirm the results, two complementary techniques were used: auger electron spectroscopy (AES) and transmission electron microscopy (TEM).

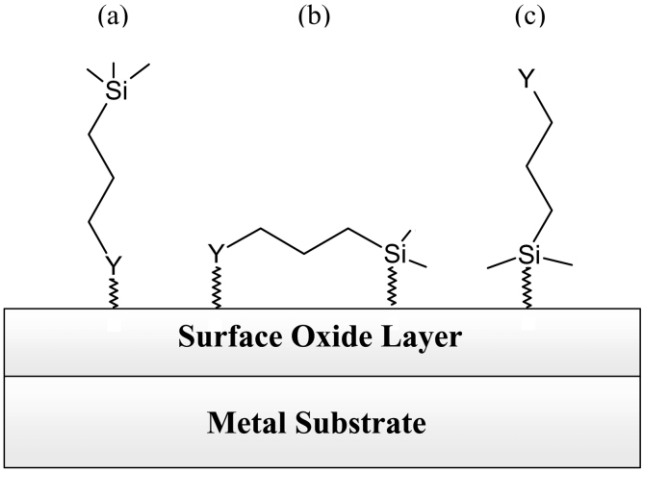

Fig. 1. Model of possible adsorption of silane molecules on metallic surfaces. (a) surface bonding via the functional group Y; (b) surface bonding via the functional and the condensed silanol groups; (c) surface bonding via the interaction between the condensed silanol group and the metallic surface.

2. Experimental

2.1. Sample preparation

Smooth and highly reflecting electropolished Al surfaces were prepared from cold rolled 99.5% (AA 1050) aluminium sheets (0.29 wt.% Fe, 0.1% Si, 0.04% Cu, 0.002% Mn, 0.002% Ti, 0.003% Zn), cut to spade electrodes sized 2.5×10 cm^2. Special care was taken not to bend the strips. One end, with an area of 2.5×4 cm^2, was electropolished for 5 min in a 1:5 perchloric acid/ethanol mixture at 15°C and a current density of 20 A dm^{-2}. After electropolishing, the samples were thoroughly rinsed with deionised water.

BTSE solutions were prepared, in accordance with the standardised procedure already described [10], by mixing silane, acetic acid, water and methanol, in that order, to obtain a stable hydrolysed silane solution. Attention was paid to maintain the pH of the solution in the 4.5–5.0 range, which results in a maximum amount of reactive silanol groups [13] that can interact with an oxide surface. In a final step, the solution was magnetically stirred for 1 day before it was used for the pre-treatment.

Silane coatings were applied by dipping the Al samples into BTSE solutions of increasing concentration (2, 4, 6, 8 and 10 vol.%) for 100 s and subsequent blow drying with compressed air to remove the excess liquid. After coating application, one series of films was cured at 200°C for 5 min, another series was left to dry at ambient temperature.

2.2. Analysis

Spectroscopic ellipsometry measurements were done

using a J.A. Woollam Co. VASE (variable angle spectroscopic ellipsometer) working in the UV-visible-NIR (250–1700 nm) spectral range with a wavelength resolution of 10 nm at two angles of incidence (76° and 80°). The analysis areas were respectively for the two angles of incidence 76° and 80°, 0.29 cm^2 and 0.41 cm^2. All the measurements were performed with an autoretarder in the measurement configuration, which enabled to keep track of the depolarisation of the reflected beam. For the analysis of the spectra, the WVASE32 (version 3.154) software was used.

Auger analysis of the silane films was carried out using a SAM PHI 650 spectrometer with a cylindrical mirror analyser (CMA) for the auger electron detection. Measurements were performed using an incident electron beam voltage of 5 kV, the analysis area was 30×40 μm^2 and the energy resolution 0.6%. Sputter depth profiles were obtained using 3.5 kV argon ions, an ion beam current of 25 mA and Ar gas pressure of 5.10^{-8} torr, the ion gun beam spot was 3×3 mm^2. The spectra and depth profiles were analysed using the PHI multipak (version 5.0) software.

3. Results and discussion

3.1. General interpretation of the SE data and optical model description

The SE spectra of the bare electropolished substrate, the cured BTSE films formed in 6% and 10% silane solutions coated on electropolished surfaces are shown in Fig. 2. The spectra of the bare substrate reveal one feature. The continuously rising Δ spectrum has a shoulder at approximately 850 nm, which is associated with a pronounced minimum in the Ψ graph. These features are directly linked with the intrinsic optical constants of the Al, which shows an interband absorption at 1.5 eV (826 nm) that is superimposed on the continuously increasing Drude-type absorption due to free electron acceleration [14]. Application of a silane film on the Al surface gives changes in the SE spectra. In the case of the 6% BTSE film, we notice a minimum at 450 nm and a maximum at approximately 860 nm in the Ψ spectrum and a discontinuous jump from 270° to −90° at 600 nm in the Δ spectrum, due to the representation of the Δ angle. The 10% BTSE film SE spectra have multiple features including various oscillations in Ψ and Δ. The increasing number of oscillations in the spectra with increasing concentration of silane in bath is attributed to the thickening of the films as it was also observed with anodic oxide films [15,16].

To extract the thickness of the BTSE films from these SE spectra an optical model has to be built and fitted on the experimental data by using simulation and non-linear least squares regression analysis [17]. In principle, a simple model describing one layer on a reflecting substrate can be used to monitor the deposited polymer film on Al. However, this model (ambient/film/substrate) requires values for the optical constants of the BTSE film and the electropolished Al, none of which are known.

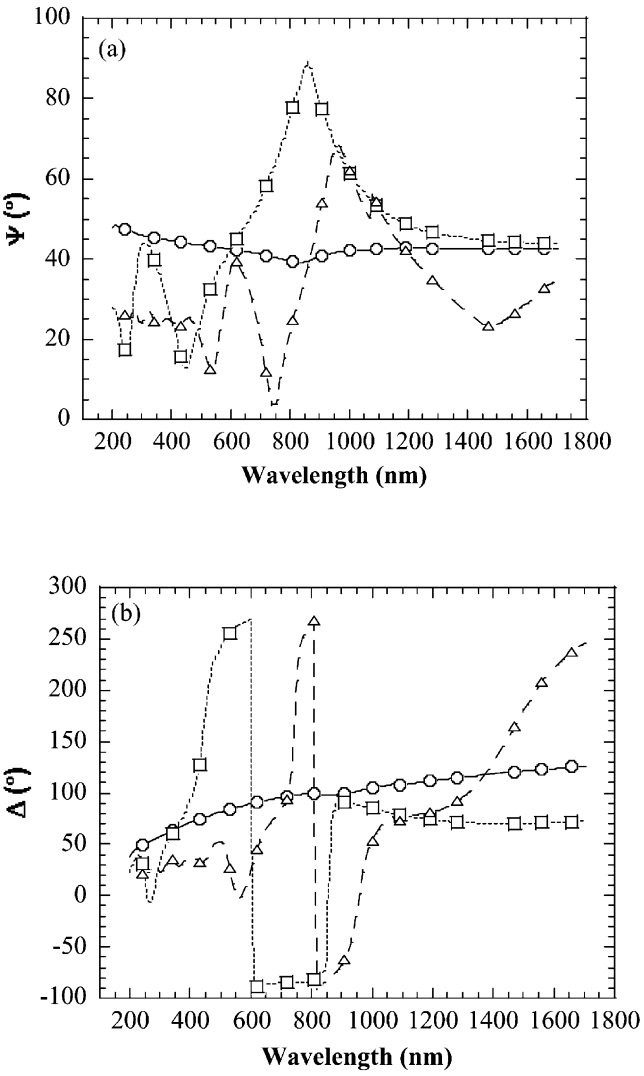

Fig. 2. Ψ (a) and Δ (b) spectra (measured at 76° incidence angle) for the bare electropolished substrate (-○-) and the electropolished surfaces covered by a cured silane film formed in 6% (-□-) and 10% (-△-) BTSE solution.

The problem of the unknown substrate optical constants has been resolved by measuring the bare electropolished surface. The sample surface such created could be equated with the situation it would be in right before the silane layer application. Based on the measured Ψ and Δ values, the real and imaginary parts of the complex index of refraction $n + ik$ were calculated and allocated to the corresponding wavelength. In this way, the optical behaviour of the substrate, expressed in terms of pseudo constants, could be simulated at each wavelength of the impinging light beam.

Because the optical constants of the BTSE layer are not known as a function of the wavelength, they are described by a dispersion relation with parameters that are determined in the modelling. A Cauchy dispersion relation [18] (valid for a transparent material in the used spectral range) has been applied to model the index of refraction of the silane film:

$$n(\lambda) = A + B/\lambda^2/ + C/\lambda^4 \quad (2)$$

$$k = 0$$

A, B and C are the dispersion parameters to be fitted and λ represents the wavelength of the light in microns. The model above described is represented in Fig. 3. The results obtained after regression for the cured film formed in 6% BTSE solution are given in Table 2. The measured and calculated Ψ and Δ spectra are shown in Fig. 4. Clearly, for both Ψ and Δ spectra, the simulated data do not match the experimental ones. In the Ψ spectrum, the maximum at 860 nm is less broad in the simulation and the two first minima (at 250 and 450 nm) are not reached by the calculation, which reveals much smaller amplitudes. In the Δ representation, other features are not perfectly modelled. The phase jumps (at 600 and 860 nm) appear less abrupt in the measured spectrum compared to the fitted one. Since Δ is closely related to the optical thickness of the film, the errors in the simulated Δ spectrum can be explained by a variation in the film thickness and can be corrected by using an extra parameter in the model, which permits a smoothening of the spectral features. This parameter describes the non-uniformity of the film thickness and is used to simulate layers, which do not have parallel interfaces [19,20]. In fact, if a film thickness varies over the width of the light beam, the resulting reflected beam would be partially polarised, as the beam may be divided up into slices, each of which effectively saw a film of slightly differing thickness. The value of this non-uniformity parameter defines the maximum and the minimum percentage deviations from the nominal thickness in the model. The second correction introduced in the model is an interphase layer between the metal and the Cauchy layer. This Bruggeman effective medium approximation (EMA) layer [21,22] is generally used to describe a small amount of interfacial intermixing or any roughness of the film/substrate interface. The assumption of the Bruggeman EMA theory is that small particles of different materials are intermixed. Under that approximation, the optical constants of the EMA layer can be calculated with:

Table 2
Parameter values after regression (top layer thickness, top layer dispersion constants) for the one-layer optical model used to interpret the SE spectra of the electropolished Al surface, covered by a cured silane film formed in 6% BTSE solution

Phase	Fit parameter	Parameter values	Comment
Ambient			$n(l) = 1$
Top layer	Thickness (nm)	86.1 ± 8.0	
	A	2.082 ± 0.130	Cauchy-type dispersion
	B (μm^2)	0.012 ± 0.008	
	C (μm^4)	0.005 ± 0.001	
Al substrate			Pseudo n and k

$$N_{mix} = \sqrt{\varepsilon_{mix}} \quad (3)$$

$$0 = \frac{(1-x)(\varepsilon_1 - \varepsilon_{mix})}{\varepsilon_1 + 2\varepsilon_{mix}} + \frac{x(\varepsilon_2 - \varepsilon_{mix})}{\varepsilon_2 + 2\varepsilon_{mix}} \quad (4)$$

where ε_1, ε_2 and ε_{mix} describe the dielectric constants of respectively the upper layer, aluminium substrate and the interphase layer, and x the fraction of aluminium present in the interphase layer. The EMA layer can effectively account for the kind of amplitude deviations that we can see in the Ψ spectrum. The extended model, including the Cauchy dispersion relation, the non-uniformity and the EMA layer is shown in Fig. 5. After fitting the parameters of the extended model on the experimental data, the results reported in

Table 3
Parameter values after regression (top and interphase layer thickness, top layer non-uniformity, top layer dispersion constants, interphase layer composition) for the extended (two-layer) optical model used to interpret the SE spectra of the electropolished Al surface, covered by a cured silane film formed in 6% BTSE solution

Phase	Fit parameter	Parameter values	Comment
Ambient			$n(l) = 1$
Top layer	Thickness (nm)	105.4 ± 3.2	
	Non-uniformity (%)	63.8 ± 2.2	
	A	1.677 ± 0.014	Cauchy-type
	B (μm^2)	-0.002 ± 0.003	dispersion
	C (μm^4)	0.002 ± 0.000	
Interphase layer	Thickness (nm)	20.1 ± 1.8	Effective medium approximation
	Al concentration (%)	11.7 ± 2.6	(Cauchy and Al)
Al substrate			Pseudo n and k

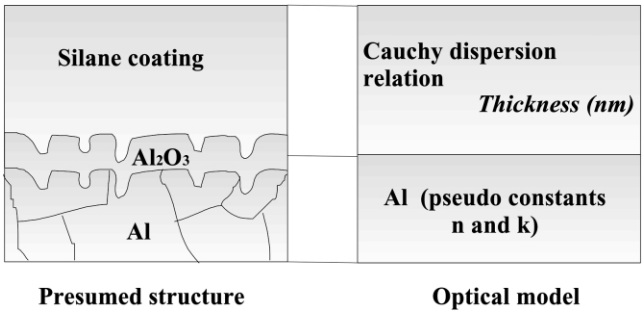

Fig. 3. One layer optical model used for the simulation of the SE measurements and for the determination of the silane layer optical constants and film thickness.

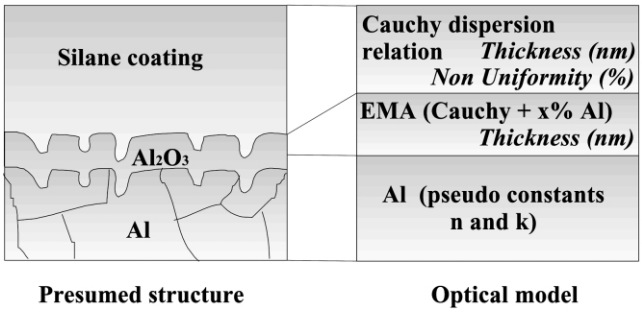

Fig. 5. Two-layer optical model used for the simulation of the SE measurements and for the determination of the silane layer optical constants, film thickness and non-uniformity.

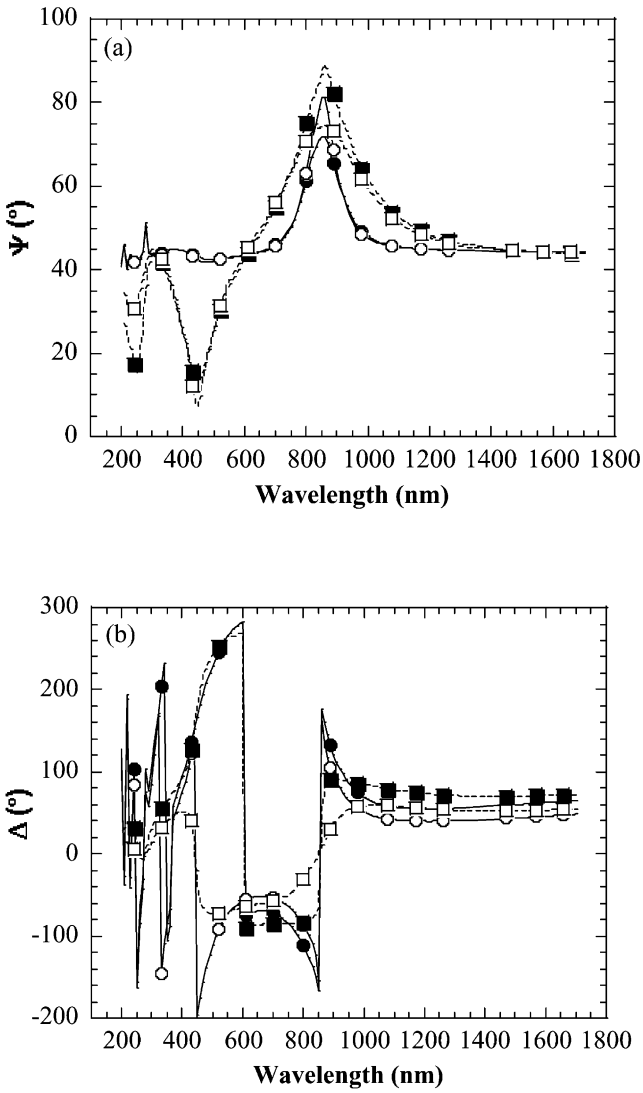

Fig. 4. Ψ (a) and Δ (b) spectra for the electropolished surface covered by a cured silane film formed in 6% BTSE solution (-■- measured at 76° incidence angle and -□- measured at 80° incidence angle) and the resulting fit obtained with the one-layer model (-●- and -○-, respectively for 76° and 80° incidence angles).

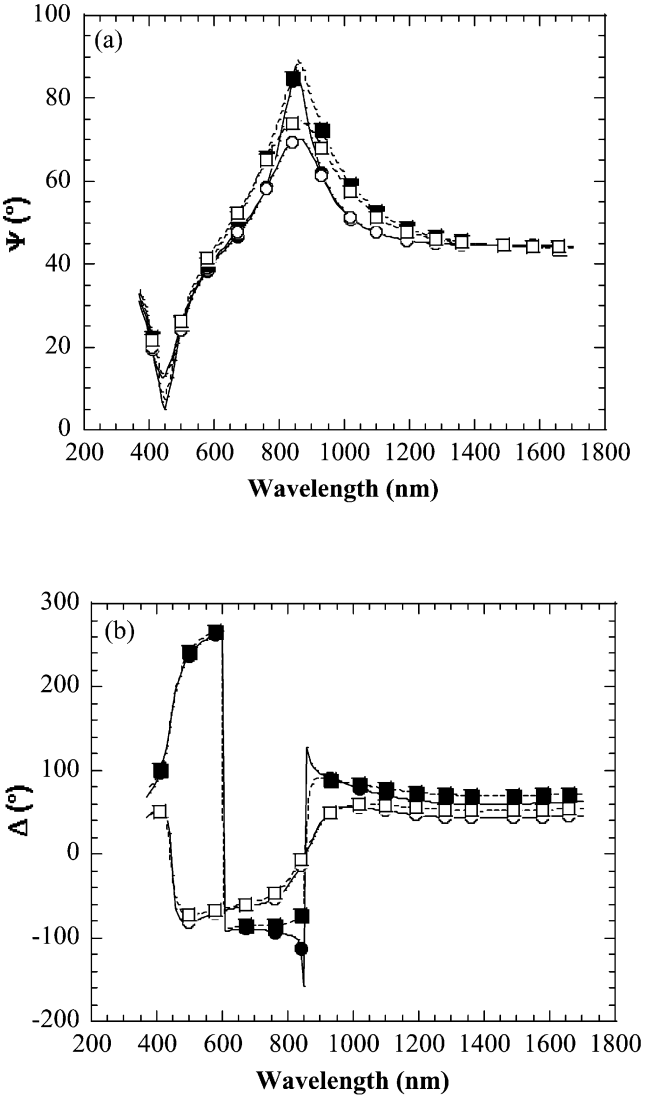

Fig. 6. Ψ (a) and Δ (b) spectra for the electropolished surface covered by a cured silane film formed in 6% BTSE solution (-■- measured at 76° incidence angle and -□-measured at 80° incidence angle) and the resulting fit obtained with the two-layer model (-●- and -○-, respectively for 76° and 80° incidence angles).

Table 3 were obtained. The measured and calculated Ψ and Δ are displayed as a function of the wavelength in Fig. 6. Directly, we can see that the introduction of these two extra parameters (EMA and non-uniformity) permits a better simulation of the experimental data. In the Ψ spectrum, the maximum (at 860 nm) and the minimum (at 450 nm) are now almost totally reproduced by the fitting. Likewise, the phase jumps apparent in the Δ spectrum and which were not simulated with the first model are well represented with the two-layer model. The thickness of the top layer is now higher (105.4 nm) compared to the value found with the first fitting (86.1 nm) but a more accurate thickness is expected considering the better correspondence between the simulation and the measurement. The degree of non-uniformity of the top layer is very high at 63.8%, but it enables a much closer reproduction of the Δ features that cannot be simulated by any other parameter. This high level of non-uniformity can be explained by the fact that the silane layer is coated on an electropolished Al without any further treatment of the metallic surface before the silane application. In other studies, like in the case of bis(3-triethoxysilylpropyl) tetrasulfane silane coatings deposited on alkaline cleaned electropolished Al, the degree of non-uniformity is smaller at approximately 15% [23]. The EMA thickness seems quite large at approximately 20 nm, however, this value is not unexceptional compared to what has been found previously for other conversion films on Al [24,25].

3.2. BTSE bath concentration influence

SE data were obtained on a series of electropolished Al surface covered by a cured (200°C, 5 min) silane coating formed in different BTSE bath concentrations (2, 4, 6, 8 and 10 vol.%) and interpreted using the same previous two-layer model. The results have been achieved using a multiple sample analysis of the measurements of the entire series. The application of this new interpretation approach is valid if two or more samples have some physical property in common. The regression on the measurements obtained from all samples is performed simultaneously, with the common physical property coupled across the models for the different samples [26]. For the samples studied in this work, infra red spectroscopic ellipsometry (1.6–40 μm) showed that if the curing conditions (temperature and time) are kept constant, the formed films are identical in composition and chemistry. This is confirmed by the obtained top layer optical constants (described by the Cauchy dispersion relation $A = 1.677$, $B = -2.10^{-3}$ μm^2, $C = 2.10^{-3}$ μm^4 and measured by UV-Vis-NIR SE) which are invariable throughout the entire series. Consequently, this multiple sample analysis was performed on all the series of identical curing conditions, allowing only the top layer thicknesses, non-uniformities and interphase layers to change. The measurements were done with two angles of incidence for each sample, which double the number of data points in the set for the analysis and thus enhance the quality of the fit. The fit results for this oven-cured series are given in Table 4. The thickness of the top layer, associated with the BTSE coating thickness, increases clearly as a function of the BTSE bath concentration (column 2) and is typically comprises between 27.1 ± 9.1 and 482.5 ± 7.1 nm. The degree of spreading of the film thickness is generally large, ranging from 39.8% to 100% and reveals an inversely proportional trend with the BTSE concentration in the bath. However, the absolute film thickness variation is always very large and more or less independent of the concentration, so it can be concluded that the deposition procedure of the silane film as it has been applied here yields intrinsically very non-uniform coatings. This is also supported by the wide spectrum of interference colours that are readily visible for the thicker films. Finally, with the exception of the sample covered by a silane film formed in the 2% solution that was the most difficult to fit due to the lack of major spectral features, the interphase layer has constant characteristics (thickness and Al concentration) within the displayed uncertainly limits throughout the entire series.

Table 4
Parameter values after regression (top and interphase layer thickness, top layer non-uniformity, interphase layer composition) for the two-layer optical model used to interpret the SE spectra of the electropolished Al surface, covered by oven-cured silane film formed in solutions with increasing BTSE bath concentration

BTSE bath concentration and curing conditions	Top layer		Interphase layer	
	Thickness (nm)	Non-uniformity (%)	Thickness (nm)	Al concentration (%)
2%, 200°C, 5 min	27.1 ± 9.1	100.0	2.1 ± 4.8	32.1 ± 39.0
4%, 200°C, 5 min	90.0 ± 3.3	100.0	18.8 ± 3.3	8.2 ± 2.1
6%, 200°C, 5 min	105.4 ± 3.2	63.8	20.2 ± 1.8	11.7 ± 2.6
8%, 200°C, 5 min	239.8 ± 4.2	45.9	18.5 ± 1.0	27.8 ± 10.9
10%, 200°C, 5 min	482.5 ± 7.1	39.8	18.2 ± 0.5	27.6 ± 5.7

Table 5
Parameter values after regression (top and interphase layer thickness, top layer non-uniformity, interphase layer composition) for the two-layer optical model used to interpret the SE spectra of the electropolished Al surface, covered by silane films formed in solutions with increasing BTSE bath concentration and left to dry at room temperature

BTSE bath concentration	Top layer		Interphase layer	
	Thickness (nm)	Non-uniformity (%)	Thickness (nm)	Al concentration (%)
2%	26.9 ± 3.7	100.0	–	–
4%	88.1 ± 1.6	75.8	12.5 ± 7.8	17.7 ± 4.3
6%	174.9 ± 3.6	68.1	15.6 ± 7.2	32.1 ± 18.0
8%	213.7 ± 2.3	33.8	14.3 ± 0.5	20.7 ± 2.6
10%	344.6 ± 4.0	36.9	16.4 ± 0.6	17.9 ± 2.3

3.3. Curing effect

As a final experiment, the effect of the curing on the film properties has been investigated. To this end, a second identical set left to dry at room temperature has been prepared and compared to the oven-cured series. The interpretation was performed using the multiple sample analysis and the two-layer model. The results for the non-oven-cured series are presented in Table 5. The interphase layer thickness is constantly small and of a similar order of magnitude for both series (column 4 in Tables 4 and 5), which indicates an interphase structure independent of the curing. The same interpretation can be deduced from the non-uniformity of the top layer, for which a downward trend with increasing BTSE bath concentrations and comparable values for both series are noticed (column 3 in Tables 4 and 5). Concerning the thickness of the silane coating itself, there is no visible systematic influence of the curing. The most important observation relates to the optical constants of the silane coating itself. In both series, a Cauchy dispersion relation was used to simulate the n and k optical constants of the top layer. As presented before, three parameters (A, B and C) must be defined and fitted. The values of these parameters for both oven-cured and uncured series are reported in Table 6. The representation of the optical constants as a function of the wavelength is reported in Fig. 7. Compared to the uncured series, the oven-cured one reveals a higher index of refraction. This result can be explained by the formation of silane films with a denser structure induced by the curing. In another study, an identical interpretation was proposed for EIS and ToF-SIMS measurements [27].

Table 6
Cauchy dispersion relation parameters for the oven-cured and for the room temperature dried series

Cauchy parameters	Oven-cured series	Room temperature dried series
A	1.677 ± 0.014	1.557 ± 0.010
B (μm^2)	−0.002 ± 0.003	0.015 ± 0.002
C (μm^4)	0.002 ± 0.000	0.003 ± 0.000

3.4. Correlation SE / AES / TEM

In order to evaluate the accuracy of the SE results, AES depth profiles and TEM micrographs of the non-cured silane coated electropolished Al samples were performed.

The TEM micrographs in Fig. 8 give an overview of the non-cured film formed in a 8 vol.% BTSE solution. These two micrographs were taken at two different places of the same sample. On both micrographs, the film/substrate interface is slightly rough and the silane coating homogeneous. However, the thickness of the silane film is very different when moving from one place of the sample to another one. The big variation of the silane film thickness directly visible in these TEM measurements can be considered as a certification of the validity of the non-uniformity parameter included in the two-layer optical model used to interpret the SE data.

The series formed by dipping the electropolished Al samples into BTSE solutions of increasing silane concentrations and left to dry at ambient temperature was analysed by AES. The depth profiles show constant

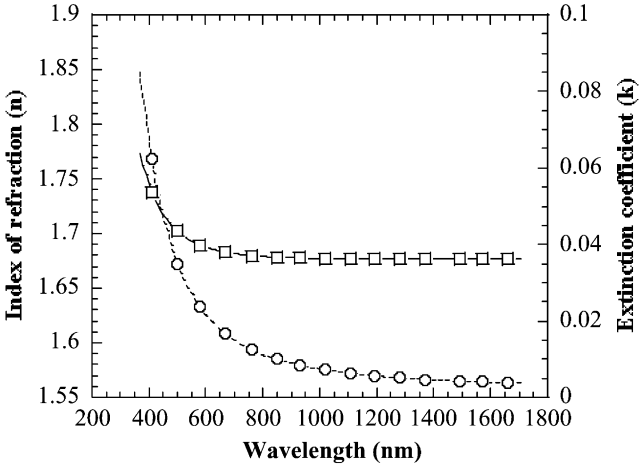

Fig. 7. Cauchy optical constants evolution as a function of the wavelength for the oven-cured (-□-) and the room temperature dried (-○-) series (the extinction coefficient is equal to 0 for both series).

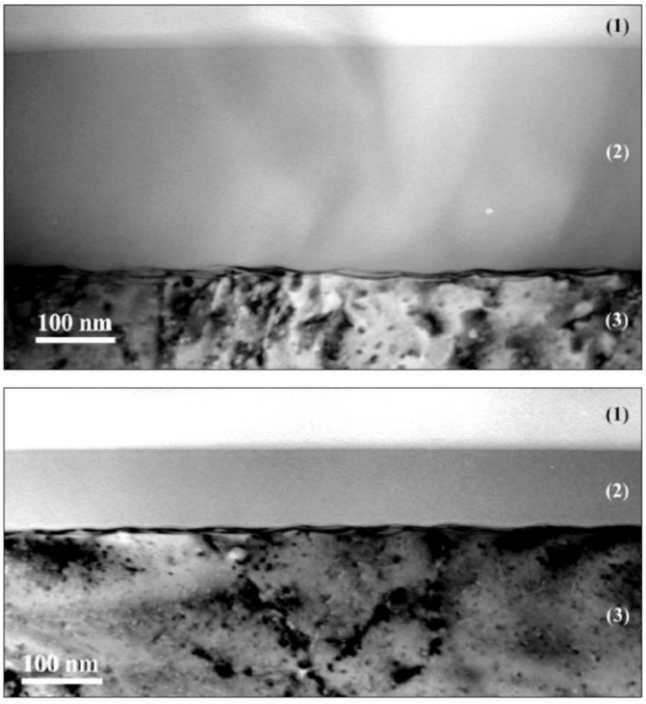

Fig. 8. Transmission electron microscopy micrographs of BTSE (8 vol.%, room temperature dried series) coating on electropolished Al sample: (1) epoxy, (2) BTSE layer, (3) aluminium.

concentrations of C, O and Si in the silane layer. After a certain sputtering time, the concentrations of C, O and Si drop to a minimum and at the same time, the metallic Al concentration becomes maximum. This indicates that the interface region is reached. In order to determine the sputtering time needed to remove the BTSE film, the Al KLL signal was employed as a criterion. The exact sputtering time was evaluated at the intersection at half of the maximum atomic concentration of the metallic element [28].

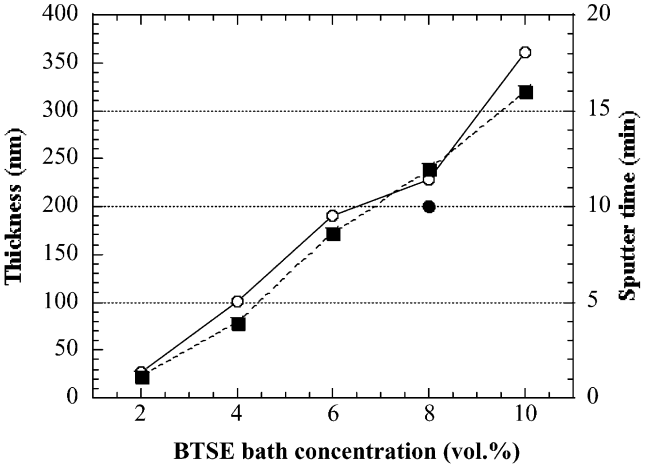

Fig. 9. Thickness (determined by -○- SE and ● TEM) and sputter time (from -■- AES depth profiles) as a function of the BTSE bath concentration.

The thickness and sputtering time, respectively from TEM analysis and AES depth profiles, are plotted as a function of the silane bath concentration and compared with the thicknesses obtained by SE on Fig. 9. The good correlation between the two curves and the TEM value shows the validity and the accuracy of the optical characterisation.

4. Conclusions

This study shows that spectroscopic ellipsometry has the potential to characterise silane coatings on aluminium substrates.

This technique is useful to determine layer thickness. To this end, an optical model that is physically realistic for the presumed surface structure has to be used. This model contains a Cauchy dispersion relation in order to describe the optical constants of the silane layer. Moreover, the addition of non-idealities, such as film thickness non-uniformity and film/substrate interphase layer (defined by a Bruggeman effective medium approximation), greatly improves the quality of the model fit. It is shown that by increasing the BTSE bath concentration, the thickness of the films is increasing significantly. The accuracy of the SE results is confirmed by additional AES and TEM analyses.

It is also demonstrated that SE can be used to study the effect of silane films curing. The higher index of refraction, deduced from SE measurements is interpreted by the creation of a denser film structure of the BTSE layer induced by the curing of the coated samples.

Acknowledgements

A. Franquet is indebted to the inter university attraction pole (PAI/IUAP 4/10) 'reduced dimensionality systems' for his fellowship. J. De Laet acknowledges the fund for scientific research (FWO) for sponsoring a visit to the University of Lincoln, Nebraska, USA. The ellipsometry equipment and T. Schram's fellowship are sponsored by the Flemish institute for the promotion of scientific-technological research in the industry (IWT). R. Beanland (UK) is acknowledged for performing the TEM analysis.

References

[1] E. Plueddemann, Silane Coupling Agents 2nd ed., Plenum Press, New York, 1990.
[2] M.J. Collie (Ed.), Corrosion Inhibitors Development since 1980, Noyes, Park Ridge, NJ, 1983, p. 182.
[3] M. Gettings, A.J. Kinloch, J. Mater. Sci. 12 (1977) 2511.
[4] Y.L. Leung, M.Y. Zhou, P.C. Wong, K.A.R. Mitchell, T. Foster, Appl. Surf. Sci. 59 (1992) 23.
[5] Y.L. Leung, Y.P. Yang, P.C. Wong, K.A.R. Mitchell, T. Foster, J. Mater. Sci. Lett. 12 (1993) 844.
[6] W.J. van Ooij, A. Sabata, J. Adhes. Sci. Technol. 5 (1991) 843.

[7] J.S. Quinton, P.C. Dastoor, Meeting Abstracts of ECASIA'99 Conference, Sevilla, Spain, October 4–8, 1999, p. 347.
[8] V. Subramanian, W.J. van Ooij, Corrosion 54 (1998) 204.
[9] B.C. Zhang, Ph.D. Thesis, University of Cincinnati, USA, 1997.
[10] W.J. van Ooij, J. Song, V. Subramanian, ATB Metallurgy 37 (1997) 137.
[11] T.F. Child, W.J. van Ooij, Trans. Inst. Met. Finish. 77 (1999) 64.
[12] R.W. Collins, D.E. Aspnes, E.A. Irene (Eds.), Spectroscopic Ellipsometry, Proceedings of the Second International Conference on Spectroscopic Ellipsometric, Charleston, South Carolina, USA, May 12–15, 1997.
[13] Z. Pu, W.J. van Ooij, J.E. Mark, J. Adhes. Sci. Technol. 11 (1997) 29.
[14] D.Y. Smith, E. Shiles, M. Inokuti, in: E. Smith (Ed.), Handbook of Optical Constants of Solids, vol. 1, Academic Press, New York, NY, 1982, p. 369.
[15] J. De Laet, J. Vanhellemont, H. Terryn, J. Vereecken, Thin Solid Films 223 (1993) 58.
[16] J. De Laet, H. Terryn, J. Vereecken, Thin Solid Films 320 (1998) 241.
[17] J. De Laet, H. Terryn, J. Vereecken, J. Vanhellemont, Surf. Interface Anal. 19 (1992) 445.
[18] M. Born, E. Wolf, Principles of Optics, Pergamon Press, Oxford, 1975.
[19] G.E. Jellison, Jr., Thin Solid Films 234 (1993) 416.
[20] U. Rossow, Thin Solid Films 313-314 (1996) 97.
[21] D.A.G. Bruggeman, Anal. Phys. 5 (1935) 636.
[22] D.E. Aspnes, Thin Solid Films 89 (1982) 249.
[23] T. Van Schaftinghen, M.S. Thesis, Vrije Universiteit Brussel, Brussels, Belgium, 1999.
[24] T. Schram, J. De Laet, H. Terryn, Thin Solid Films 313-314 (1998) 728.
[25] T. Schram, J. De Laet, H. Terryn, Thin Solid Films 145 (1998) 2733.
[26] K. Järrendahl, H. Arwin, Thin Solid Films 313-314 (1998) 114.
[27] A. Franquet, H. Terryn, J. Vereecken, P. Bertrand, A. Delcorte, Meeting Abstracts of ECASIA'99 Conference, Sevilla, Spain, October 4–8, 1999, p. 344.
[28] D. Briggs, M.P. Seah, in Wiley (Ed.), Practical Surface Analysis, 2nd ed., New York NY, 1990, p. 158.